



# A variable polarisation compensator using artificial dielectrics

David R.S. Cumming<sup>\*</sup>, Richard J. Blaikie

*Department of Electrical and Electronic Engineering, University of Canterbury, Private Bag 4800, Christchurch, New Zealand*

Received 16 December 1998; received in revised form 9 March 1999; accepted 13 March 1999

## Abstract

Artificial dielectrics can be made to exhibit strong birefringence. This property may be used to construct waveplates for a variety of applications. In this article, a method for making a variable artificial dielectric retarder, akin to a Babinet–Soleil compensator, is investigated. Whilst the feature sizes are too small for this device to be practical at optical wavelengths, the technique lends itself to quasi-optical instruments operating at terahertz wavelengths. © 1999 Elsevier Science B.V. All rights reserved.

PACS: 42.81.GS; 42.79.Ry; 42.79. – e

Keywords: Birefringence; Artificial dielectrics; Polarisation

## 1. Introduction

Artificial dielectrics are now widely used to reduce reflections at optical surfaces. Many authors have studied this so-called ‘moth-eye’ effect [1]. One example of an artificial dielectric is a dense array of pyramid-like structures patterned into the surface of an optical device. To a first approximation, provided the period of the array is less than  $\lambda_0/4$  ( $\lambda_0$  is the wavelength in free space), then the surface pattern will appear as a continuous film with a graded dielectric constant between the external medium and the substrate dielectric. It is the grading of the apparent refractive index that gives rise to the reduction in the reflection coefficient [2].

If instead of a two-dimensional array, a linear grating is made to modulate the surface profile, then the apparent dielectric constant as a function of depth will be different for light polarised parallel or perpendicular to the grating. For the purpose of constructing anti-reflection surfaces, this can be a disadvantage, but the modification to the

polarisation of the transmitted ray is of use in the fabrication of waveplates. This property is studied with a view to constructing a variable waveplate.

The device is composed of two artificial dielectrics with identical surface profiles. When the two plates are turned to face each other, the surface profiles of each device will interlock. We have modeled the operation of the device in three ways: completely analytically (with restrictions), quasi-analytically with no restrictions, and numerically. In this way we have been able to arrive at a better than qualitative understanding of how the device works and subsequently improve the accuracy of our calculations. We predict that for a device made of silicon, operating at 1 THz, a phase retardation between 0 and 60° can be achieved for a change in plate separation of only 35  $\mu\text{m}$ .

## 2. Effective medium theory

In this section we will consider an analytical model for the operation of the proposed device. Fig. 1 is a sketch of an artificial dielectric grating with a triangular profile. The cross-section is symmetric and triangular with a period  $P$  and a depth  $d$ . Radiation that is incident along the normal to the surface can be resolved into components polarised

<sup>\*</sup> Corresponding author. Present address: Department of Electronics and Electrical Engineering, Nanoelectronics Research Centre, University of Glasgow, Glasgow G12 8QQ, UK. E-mail: d.cumming@elec.gla.ac.uk

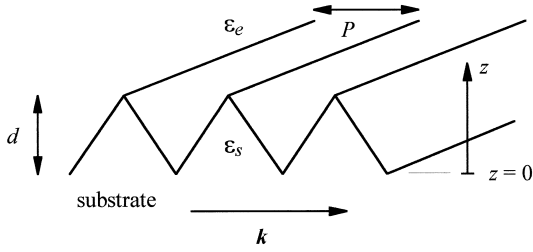


Fig. 1. A one-dimensional artificial dielectric with a triangular surface profile.

parallel or perpendicular to the grating with electric field  $E \parallel k$  and  $E \perp k$ , respectively, where  $k$  is the grating vector. The effective dielectric constant at any depth,  $z$ , can be calculated using effective medium theory (EMT) [3]. First, the fill-factor,  $f(z)$ , is found to be

$$f(z) = 1 - \frac{z}{d} \quad (0 < z \leq d). \quad (1)$$

For radiation with  $E \perp k$ , the zeroth order approximation of the effective dielectric constant is given by

$$\varepsilon_{\perp}^{(0)}(z) = \varepsilon_s f(z) + \varepsilon_e (1 - f(z)) \quad (2)$$

where  $\varepsilon_s$  is the dielectric constant of the substrate, and  $\varepsilon_e$  is the dielectric constant of the external medium. Similarly, for light propagating with  $E \parallel k$ , the effective dielectric constant is

$$\varepsilon_{\parallel}^{(0)}(z) = \left[ \frac{f(z)}{\varepsilon_s} + \frac{1 - f(z)}{\varepsilon_e} \right]^{-1}. \quad (3)$$

Clearly, transmitted radiation with  $E \perp k$  or  $E \parallel k$  will experience different effective dielectric constants (birefringence), thus there will be a polarisation change for radiation transmitted through the structure.

An improved estimate of the effective dielectric constants can be calculated using second order EMT [4], such that

$$\varepsilon_{\perp}^{(2)} = \varepsilon_{\perp}^{(0)} \left[ 1 + \frac{1}{3\varepsilon_0 \varepsilon_{\perp}^{(0)}} \times \left( \pi(\varepsilon_s - \varepsilon_e) \frac{P}{\lambda_0} f(z)(1 - f(z)) \right)^2 \right] \quad (4)$$

and

$$\varepsilon_{\parallel}^{(2)} = \varepsilon_{\parallel}^{(0)} \left[ 1 + \frac{\varepsilon_{\perp}^{(0)}}{3\varepsilon_0} \times \left( \pi \frac{\varepsilon_{\parallel}^{(0)}(\varepsilon_s - \varepsilon_e)}{\varepsilon_e \varepsilon_s} \frac{P}{\lambda_0} f(z)(1 - f(z)) \right)^2 \right]. \quad (5)$$

Fig. 2 is a diagram of the novel variable polarisation compensator that is proposed in this article. It consists of two artificial dielectrics with surface profiles that interlock

with each other, and a separation  $s$ . When  $s = 0$ , there will be no artificial dielectric, thus no birefringence. When the two plates are separated by an amount  $s < d$ , there will exist an artificial dielectric with a fill-factor that must be calculated in three regions, thus

$$f(z) = \begin{cases} 1 - \frac{z}{d} & (0 \leq z < s) \\ 1 - \frac{s}{d} & (s < z \leq d) \\ 1 - \frac{z - s}{d} & (d < z \leq s + d) \end{cases} \quad (6)$$

As for the simple grating,  $\varepsilon_{\perp}(z)$  and  $\varepsilon_{\parallel}(z)$  for the two-plate structure are calculated using the fill-factor and the equations described above.

The optical path length for either polarisation will be varied with  $s$ , and this is akin to the operation of a Babinet–Soleil compensator [5]. To calculate the phase shift experienced by each polarisation in the device it is necessary to calculate the effective propagation constant of the artificial dielectric. The effective index of refraction is given by  $n(z) = \sqrt{\varepsilon_r(z)}$ , where  $\varepsilon_r$  is the effective dielectric constant, for either polarisation. The integrated propagation constant that is used to calculate the overall phase shift experienced on transmission through an artificial dielectric will therefore be

$$k_{u,v} = \frac{k_0}{v - u} \int_u^v n(z) dz \quad (7)$$

where  $v$  and  $u$  define the boundaries of the portion of the artificial dielectric concerned.  $k_0$  is the propagation constant in free space.

For the proposed device, Eqs. (6) and (7) are evaluated in each of the three regions as a function of  $s$  for both  $E \perp k$  and  $E \parallel k$ . The phase shift between  $E \perp k$  and  $E \parallel k$  when  $s < d$  is then calculated to be

$$\Delta\phi_{s < d}(s) = (k_{0,s}^{\perp} - k_{0,s}^{\parallel})s + (k_{s,d}^{\perp} - k_{s,d}^{\parallel})(d - s) + (k_{d,s+d}^{\perp} - k_{d,s+d}^{\parallel})s \quad (8)$$

by accumulating the phase shift in the three regions. This simple analysis, which we will refer to as the EMT<sup>(n)</sup> model can be applied to both zeroth and second order calculations of the dielectric constant ( $n$  is the order). However, it does not account for reflections between the

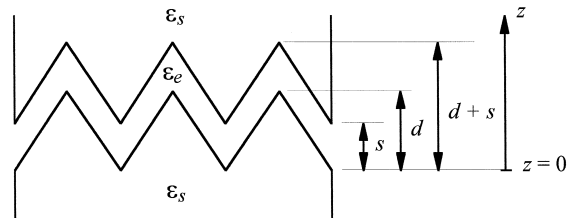


Fig. 2. A cross-section through the proposed compensator showing the dimensions of the device when  $s < d$ .

plates, and it cannot deal with  $s > d$ . A somewhat more sophisticated, pseudo-analytical, model is required to do this and we will discuss it in Section 3.

### 3. Effective medium theory in a Fabry–Perot cavity

The model presented in Section 2 is inadequate since it fails to account for internal reflections between the two plates of the compensator. It can be seen from Eq. (6) that when  $s < d$  the fill-factor in the central region of the proposed device is a constant for a given separation. The structure may then be viewed as a Fabry–Perot (FP) cavity with an internal medium composed of an artificial dielectric of invariant fill-factor, and end-faces that are composed of graded artificial dielectric on the surface of a solid dielectric. A similar model can be developed for  $s > d$ . We will refer to these models as the EMT<sup>(n)</sup> + FP model.

As for a simple cavity, the transmission coefficient for the complete structure may be modeled as the sum of internally reflected terms with magnitude that diminishes to zero as the number of reflections approaches infinity. The overall transmission coefficient is therefore the sum of a geometric series that converges to a finite value. For the variable compensator, there will be a phase shift, due to the graded artificial dielectric end-faces, associated with each reflection (see Fig. 3) and, correspondingly, for the transmitted radiation.

It can be shown that when  $s < d$ , the transmission coefficient through the complete structure for the perpendicular polarisation is

$$T_{s < d}^{\perp} = \frac{t_{0,s}^{\perp} t_{d,d+s}^{\perp} e^{i(k_{d,s}^{\perp}(d-s) + k_{\text{SUB}} s)}}{1 - (r^{\perp})^2 e^{2ik_{d,s}^{\perp}(d-s)}} \quad (9)$$

where  $t_{0,s}^{\perp}$  is the transmission coefficient for radiation entering the cavity and  $t_{d,d+s}^{\perp}$  is the transmission coefficient

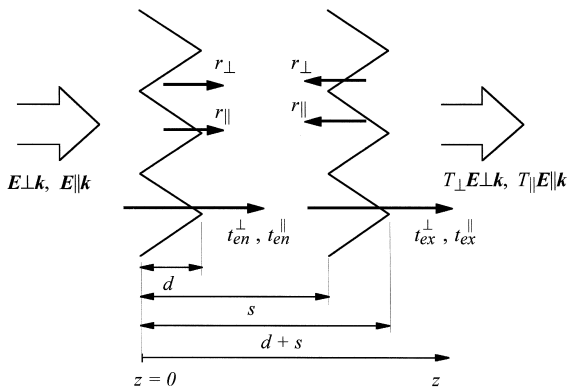


Fig. 3. The distances and coefficients used to determine the transmission properties of the proposed device when  $s > d$ .  $t_{\text{en}}$  and  $t_{\text{ex}}$  denote the transmission coefficient for radiation entering and exiting the cavity, respectively. The coordinate system in use is also shown.

for radiation leaving the cavity. The subscript letters denote the boundaries of the artificial dielectric layers for which the coefficients are calculated.  $r^{\perp}$  is the reflection coefficient inside the cavity, and is assumed to be the same at each end—i.e.,  $r_{s,0}^{\perp} = r_{d,d+s}^{\perp} = r^{\perp}$ .  $k_{d,s}^{\perp}$  is the integrated propagation constant in the central region of the structure where  $f(z)$  is invariant with  $s$ .  $k_{\text{SUB}}$  is the propagation constant in the device substrate. To simplify the model, the effect of reflections from the unpatterned back faces of the two substrates, used to implement such a device, is ignored.

When  $s > d$ , the transmission coefficient when  $E \perp k$  is

$$T_{s > d}^{\perp} = \frac{t_{0,d}^{\perp} t_{d+s,2d+s}^{\perp} e^{i(k_0 s + k_{\text{SUB}} d)}}{1 - (r^{\perp})^2 e^{2ik_0(s-d)}} \quad (10)$$

Note that Eqs. (9) and (10) use the coordinate system of Figs. 2 and 3, with all distance parameters referred to  $z = 0$ . The subscripts adhere to this system. When  $s = d$ , Eqs. (9) and (10) are identical, as one would expect.

Equations for  $T^{\parallel}$ , equivalent to Eqs. (9) and (10), for parallel polarised radiation can also be calculated. By extracting the phase term from each transmission coefficient, the difference in the phase shift between polarisations as a function of  $s$  can be calculated. When  $s < d$ , it is found to be

$$\begin{aligned} \Delta \phi_{s < d}(s) &= (\phi_{0,s}^{\perp} + \phi_{d,d+s}^{\perp}) - (\phi_{0,s}^{\parallel} + \phi_{d,d+s}^{\parallel}) \\ &\quad - \tan^{-1} \left[ \frac{|r^{\perp}|^2 \sin \theta_{s < d}^{\perp}}{1 - |r^{\perp}|^2 \cos \theta_{s < d}^{\perp}} \right] \\ &\quad + \tan^{-1} \left[ \frac{|r^{\parallel}|^2 \sin \theta_{s < d}^{\parallel}}{1 - |r^{\parallel}|^2 \cos \theta_{s < d}^{\parallel}} \right] \end{aligned} \quad (11)$$

where  $\theta_{s < d}^{\perp} = \phi_{s < d}^{\perp} + 2k_{d,s}^{\perp}(d-s)$  and  $\theta_{s < d}^{\parallel} = \phi_{s < d}^{\parallel} + 2k_{d,s}^{\parallel}(d-s)$ . Similarly, when  $s > d$ , it can be shown that

$$\begin{aligned} \Delta \phi_{s > d}(s) &= (\phi_{0,d}^{\perp} + \phi_{d+s,2d+s}^{\perp}) - (\phi_{0,d}^{\parallel} + \phi_{d+s,2d+s}^{\parallel}) \\ &\quad - \tan^{-1} \left[ \frac{|r^{\perp}|^2 \sin \theta_{s > d}^{\perp}}{1 - |r^{\perp}|^2 \cos \theta_{s > d}^{\perp}} \right] \\ &\quad + \tan^{-1} \left[ \frac{|r^{\parallel}|^2 \sin \theta_{s > d}^{\parallel}}{1 - |r^{\parallel}|^2 \cos \theta_{s > d}^{\parallel}} \right] \end{aligned} \quad (12)$$

where  $\theta_{s > d}^{\perp} = \phi_{s > d}^{\perp} + 2k_0(s-d)$  and  $\theta_{s > d}^{\parallel} = \phi_{s > d}^{\parallel} + 2k_0(s-d)$ . As for Eqs. (9) and (10), Eqs. (11) and (12) match up when  $s = d$ .

To complete the analysis it is necessary to calculate the reflection and transmission coefficients ( $r$  and  $t$  parameters) to determine both their phase and magnitude. Using analytical expressions comprised of Bessel functions it is possible to generate good approximations based on Eqs. (2) and (3) (zeroth order EMT), and we have done this

using the technique of Raguin and Morris [3]. However, it is known that EMT becomes inaccurate for materials with high dielectric constant when the grating period approaches  $\lambda_0/4$ . Therefore, in order to achieve more accuracy, we have also studied the properties of the device using a numerical tool.

#### 4. Multiple-multipole method

The multiple-multipole method (MMP) is a computational technique that permits rigorous field calculations to be performed by expanding the electromagnetic field within domains as analytical series [6]. A more widely used technique for diffraction problems is rigorous coupled wave analysis (RCWA). RCWA also uses analytical expansions to match the solution at the boundaries [7]. Our choice of technique has therefore been predicated by the availability of suitable tools. MMP yields the accuracy of full numerical techniques, such as the finite difference time-domain method, but with much greater speed. MMP has therefore been employed to evaluate the proposed device. It is ideal, since it permits many different structures, representing a sweep in the plate separation,  $s$ , to be simulated in a short time.

A key consideration in using MMP is the positioning of the expansions in the simulation domains. Several types may be used but for this work only multipole, Bessel and Rayleigh expansions were required. The structure is periodic and boundaries are defined to match at the left and right hand sides of the original (one period) cell. The gap between the two triangular surface profiles is assumed to be dry air. The patterned dielectric material of each plate is assumed to extend to infinity to the left and right. The substrate for each plate is also assumed to be infinitely thick. As for the analytical calculations, this simplifies the problem by reducing the number of reflective boundaries. Each time the boundaries are moved (to increase the separation) the expansions are moved too, and the simulation repeated. The difference in phase shift between  $\mathbf{E} \perp \mathbf{k}$  and  $\mathbf{E} \parallel \mathbf{k}$  is extracted from the resultant field data and plotted. The data may also be directly extracted from the Rayleigh expansion parameters in MMP.

#### 5. Results

Fig. 4 is a typical behaviour for the proposed device, calculated both semi-analytically (EMT<sup>(n)</sup> and EMT<sup>(0)</sup> + FP) and using MMP. The conditions were for a silicon dielectric ( $\epsilon_r = 12$ ), which was assumed to be lossless. The surface profile has a period,  $P$ , of 50  $\mu\text{m}$  and a depth,  $d$ , of 35  $\mu\text{m}$ . These sizes correspond to manufacturable structures using processes based on conventional silicon micro-machining [8]. The simulation frequency for the MMP method was 1 THz, corresponding to  $\lambda_0 = 6P = 300 \mu\text{m}$ .

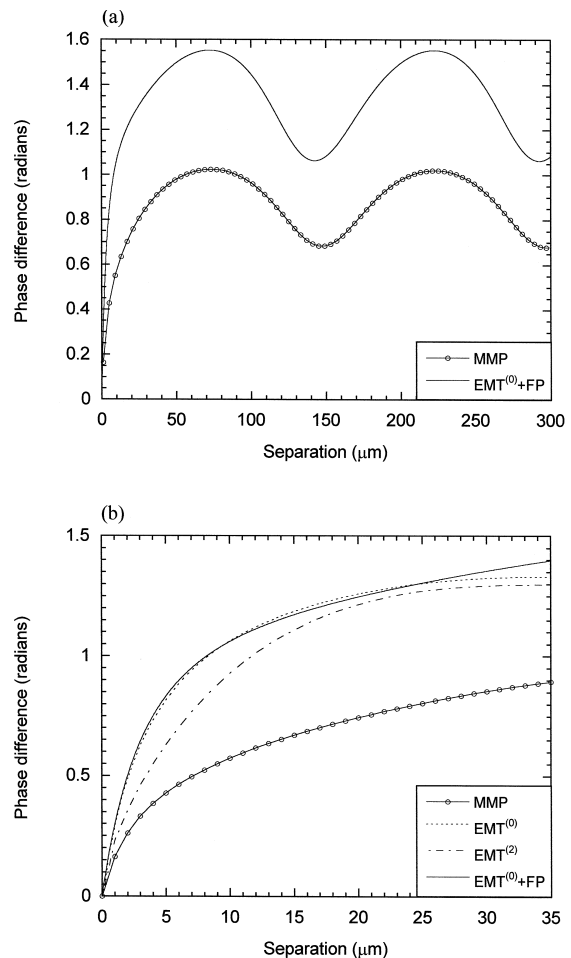


Fig. 4. (a) The calculated phase shift as a function of the plate separation of the proposed device using MMP and EMT in a FP cavity (EMT<sup>(0)</sup> + FP). (b) The calculated phase shift in the region  $s < d$ . The results for three models are shown, namely MMP, EMT<sup>(n)</sup> only (zeroth and second order) and EMT<sup>(0)</sup> + FP.

The predicted characteristic demonstrates a device in which the polarisation shift increases rapidly with plate separation when  $s < d$ . When  $s > d$ , the difference in phase shift oscillates as the path length within the cavity is modified.

There is, however, a significant discrepancy between the analytical and MMP models. This can also be seen when the transmission and reflection coefficients for the device are compared directly (see Fig. 5). It is clear that the EMT<sup>(0)</sup> + FP and MMP models are not in perfect agreement. This is because for cases where the dielectric constant of the substrate is particularly large, the analytical treatment we have employed is known to be inadequate, especially for the case where  $\mathbf{E} \parallel \mathbf{k}$  [3]. However, the elementary model, EMT<sup>(0)</sup>, compares well with the more sophisticated EMT<sup>(0)</sup> + FP model when  $s < d$  (i.e., in the EMT only model's range of validity). The second order

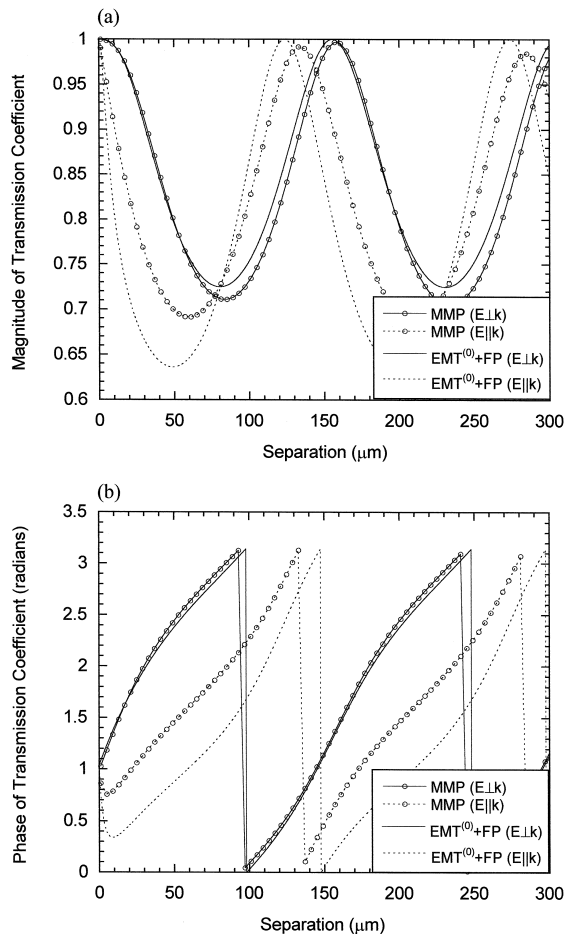


Fig. 5. (a) The magnitude and (b) the phase of the transmission coefficients  $T^\perp$  and  $T^\parallel$  of the proposed device using MMP and EMT<sup>(0)</sup>+FP.

model, EMT<sup>(2)</sup>, predicts a slightly more modest phase shift, but still does not agree well with the MMP calculation. This is at least partly due to the weakness of second order EMT in accurately calculating the effective dielectric constant for  $E\parallel k$  [9]. The problem is exacerbated by our desire to extract the phase difference—a derivative property—and not just the absolute phase, thus increasing the error. The MMP tool generates error calculations based on the goodness of the field matching at the boundaries between domains. We find that for small separations the average error is less than 1%. The error increases for large separations ( $s \gg d$ ) thus we believe that the results of the MMP simulations are of good accuracy for small separations up to three or four times the groove depth.

Fig. 5 also demonstrates the difference between the magnitudes of the two transmission coefficients for  $E \perp k$  and  $E \parallel k$ . The maximum discrepancy is approximately 0.1 for a maximum transmission of 1.0, for the conditions considered above. This difference would be a problem in constructing precise waveplates. However, this discrepancy will decrease if dielectrics with lower dielectric constant are used. The trade-off is that either structures with deeper grooves or more substrates, stacked on top of each other, will be needed to achieve the same phase shift [10].

## 6. Conclusion

A novel variable artificial dielectric retarder is proposed. Whilst the implementation of this device is impractical at optical wavelengths, it is possible to make working structures at terahertz frequencies, where the physical dimensions used are several tens of micrometres. The device has been modeled in detail. Analytical techniques have been employed to expose the underlying behaviour of the device and a numerical technique has been used to achieve greater accuracy. For the parameters considered, it is predicted that a variable phase shift from 0 up to approximately  $60^\circ$  is possible. Because it employs artificial dielectrics, power loss will be reduced due to a reduction in the reflection coefficient at the substrate/air interface. It is anticipated that the proposed device will prove useful in the development of future quasi-optical terahertz systems.

## Acknowledgements

The authors are grateful to Christian Hafner of ETH Zurich for permission to use pre-release versions of the MMP software, Max1.

## References

- [1] P.B. Clapham, M.C. Hutley, *Nature* 244 (1973) 281.
- [2] L. Rayleigh, *Proc. London Math. Soc.* 11 (1880) 51.
- [3] D.H. Raguin, G.M. Morris, *Appl. Opt.* 32 (1993) 2582.
- [4] S.M. Rytov, *Sov. Phys. JETP* 2 (1956) 466.
- [5] M. Born, E. Wolf, *Principles of Optics*, Pergamon, Oxford, 1970.
- [6] C. Hafner, *The Generalised Multipole Technique For Computational Electromagnetics*, Artech House, Boston, 1990.
- [7] T.K. Gaylord, M.G. Moharam, *Proc. IEEE* 73 (1985) 894.
- [8] D.B. Lee, *J. Appl. Phys.* 40 (1969) 4569.
- [9] D.H. Raguin, G.M. Morris, *Appl. Opt.* 32 (1993) 1154.
- [10] D.H. Raguin, S. Norton, G.M. Morris, *SPIE Proc. CR49* (1993) 234.